Unsteady Turbulence in Tidal Bores: Effects of Bed Roughness

Hubert Chanson[1]

Abstract: A tidal bore is a wave propagating upstream as the tidal flow turns to rising. It forms during spring tide conditions when the flood tide is confined to a narrow funneled channel. To date, theoretical and numerical studies rely upon physical experiments to validate the developments, but the experimental data are limited mostly to visual observations and sometimes free-surface measurements. Herein turbulent velocity measurements were obtained in a large-size laboratory facility with a fine spatial and temporal resolution. The instantaneous velocity measurements showed rapid flow deceleration at all vertical elevations, and large fluctuations of all velocity components were recorded beneath the bore and secondary waves. A comparison between undular (nonbreaking) and breaking bores suggested some basic differences. In an undular bore, large velocity fluctuations were recorded beneath the first wave crest and the secondary waves showing a long-lasting effect after the bore passage. In a breaking bore, some large turbulent stresses were observed next to the shear zone in a region of high velocity gradients, while some transient flow recirculation was recorded next to the bed. The effects of bed roughness were tested further. The boundary friction contributed to some wave attenuation and dispersion, and the free-surface data showed some agreement with the wave dispersion theory for intermediate gravity waves. The instantaneous velocity data showed however a significant effect of the boundary roughness on the velocity field next to the boundary ($z/d_o < 0.2$) for both undular and breaking bores. Overall the findings were consistent with field observations of tidal bores and highlighted the significant impact of undular (nonbreaking) bores on natural systems.

DOI: 10.1061/(ASCE)WW.1943-5460.0000048

CE Database subject headings: Turbulence; Bed roughness; Tidal currents; Wave propagation.

Author keywords: Tidal bores; Turbulence; Bed roughness; Physical modeling.

Introduction

A tidal bore is a wave propagating upstream as the tidal flow turns to rising (Darwin 1897; Barré de Saint Venant 1871; Rayleigh 1908; Tricker 1965). It forms during spring tide conditions when the flood tide is confined to a narrow funneled channel, and the leading edge of the tidal wave becomes a water depth discontinuity (Fig. 1). The best historically documented tidal bores are those of the Qiantang, Seine, and Dordogne Rivers in China and France. A related occurrence is the positive surges commonly observed in man-made channels. The inception and development of bores and surges may be predicted using the method of characteristics and Saint-Venant equations (Barré de Saint Venant 1871). After formation of the surge, the flow properties immediately upstream and downstream of the front must satisfy the continuity and momentum principles (Henderson 1966; Liggett 1994; Chanson 2004)

$$\frac{d_{\text{conj}}}{d_o} = \frac{1}{2}(\sqrt{1 + 8\mathsf{F}^2} - 1) \tag{1}$$

where d_o = initial water depth; d_{conj} = conjugate depth observed immediately after the bore passage; and F = surge Froude number defined as

$$\mathsf{F} = \frac{V_o + U}{\sqrt{g d_o}} \tag{2}$$

with V_o = initial flow velocity; g = gravity acceleration; and U = surge front celerity for an observer standing on the bank, positive upstream (Fig. 2). Eq. (1) is called the Bélanger equation (Henderson 1966; Chanson 2004).

To date, theoretical and numerical studies of tidal bores and surges rely upon some physical experiments to validate the developments (e.g., Benjamin and Lighthill 1954; Peregrine 1966; Mazumder and Bose 1995). Most experimental data were limited to visual observations and sometimes free-surface measurements (e.g., Darcy and Bazin 1865; Favre 1935; Benet and Cunge 1971; Treske 1994). Previous studies rarely encompassed turbulence measurements except in a few limited studies (Hornung et al. 1995; Koch and Chanson 2008, 2009). In the following, some turbulent velocity measurements were obtained in a large-size laboratory facility with a fine spatial and temporal resolution. Two bed roughness configurations were tested systematically, corresponding to smooth-turbulent and fully rough turbulent flow conditions. The unsteady turbulence data provide an unique description of the advancing bore front and of the turbulent mixing process. The outcomes yield some benchmarks for future theoretical and numerical models.

[1]Professor in Hydraulic Engineering, School of Civil Engineering, The Univ. of Queensland, Brisbane, QLD 4072, Australia. E-mail: h.chanson@uq.edu.au

Note. This manuscript was submitted on August 24, 2009; approved on January 13, 2010; published online on February 4, 2010. Discussion period open until February 1, 2011; separate discussions must be submitted for individual papers. This paper is part of the ***Journal of Waterway, Port, Coastal, and Ocean Engineering***, Vol. 136, No. 5, September 1, 2010. ©ASCE, ISSN 0733-950X/2010/5-247–256/$25.00.

(a)

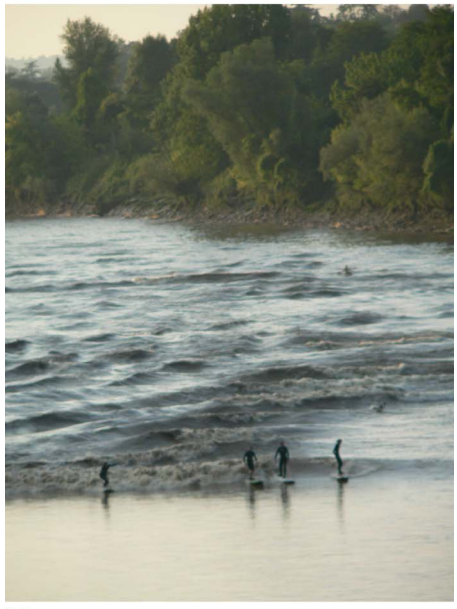

(b)

(c)

Fig. 1. Photographs of tidal bore: (a) undular tidal bore of the Dordogne River at St Pardon on the evening of July 22, 2008 (note the surfer on the right); (b) tidal bore of the Garonne River at Podensac on August 2, 2008 looking at the incoming bore front (note the surfers but also the three-dimensional nature of the tidal bore); and (c) undular tidal bore the Sélune River at Pontaubault, Baie du Mont Saint Michel on August 2, 2008

Experimental Facility and Instrumentation

Experimental Facility

The new experiments were performed in the tilting flume at the University of Queensland previously used by Koch and Chanson

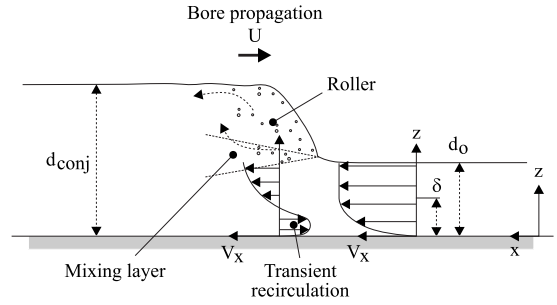

Fig. 2. Definition sketch of a breaking bore, with some transient recirculation beneath the roller

(2005) but with different flow conditions and instrumentation (Table 1, Fig. 3). The channel was 0.5 m wide and 12 m long, and its slope was horizontal. The flume was made of smooth PVC bed and glass walls, and the waters were supplied by a constant head tank. A tainter gate was located next to the channel downstream end.

For some experiments, the smooth PVC channel bed was covered with rough screens (Series 1B, Table 1). The screens were made from plastic electrical lighting louvers with square patterns (16 mm size, 1 mm thick, 8 mm high) that are seen in Fig. 3(b). The hydraulic roughness of the screens was tested in some steady open channel flow conditions. The equivalent Darcy-Weisbach friction factor ranged from $f=0.05-0.08$ corresponding to the fully rough turbulent flow regime (Schlichting 1960; Henderson 1966). The results were basically independent of the Reynolds number R and best correlated by

$$\frac{1}{\sqrt{f}} = 0.252\left(\frac{k}{D_H}\right)^{-0.823} \tag{3}$$

where k=screen height ($k=8$ mm) and D_H=hydraulic diameter. For comparison, the friction factor in turbulent channels flow may be estimated from the Colebrook-White formula (Liggett 1994; Chanson 2004)

$$\frac{1}{\sqrt{f}} = -2.0\log_{10}\left(\frac{k_s}{2.71D_H} + \frac{2.51}{\mathrm{R}\sqrt{f}}\right) \tag{4}$$

where k_s=equivalent sand roughness height. The best correlation between the rough screen data and the Colebrook-White formula [Eq. (4)] was obtained using an equivalent sand roughness height $k_s=6.6$ mm comparable to the screen thickness $k=8$ mm.

Instrumentation

The water discharge was measured with two orifice meters that were designed based upon the British Standards (1943). The percentage of error was less than 2%. The unsteady water depths were measured with a series of acoustic displacement meters Microsonic Mic+25/IU/TC which were spaced along the channel between $x=10.8$ and 2 m, where x=longitudinal distance from the channel upstream end. One such sensor is clearly visible in Fig. 3(a). The data accuracy and dynamic response of the sensors were 0.18 mm and 50 ms, respectively.

The turbulent velocity measurements were conducted with an acoustic Doppler velocimeter (ADV) Nortek Vectrino+ (Serial No. VNO 0436) using a side-looking head equipped with four receivers. For all the experiments, the ADV sampling volume was located at $x=5$ m, the velocity range was 1.0 m/s, the sampling rate was 200 Hz, and the data accuracy was 1% of the velocity

Table 1. Experimental Investigations of the Turbulent Velocity Field in Tidal Bores

Reference	S_o	Q (m^3/s)	d_o (m)	Gate opening h (m)	Bore type (at $x=5$ m)	U (m/s)	Fr	Remarks
Hornung et al. (1995)	0	0	—	N/A	Undular to breaking (+)	—	1.5–6	Smooth bed $L=24$ m
Koch and Chanson (2005, 2009)	0	0.040	0.079	0.010–0.092	Undular to breaking	0.14–0.68	1.31–1.93	Smooth PVC bed $L=12$ m, $B=0.5$ m
Present study								
Series 1A	0	0.058	0.137	0.010–0.110	Undular to breaking	0.56–0.90	1.17–1.49	Smooth PVC bed $L=12$ m, $B=0.5$ m
Series 1B	0	0.058	0.14 (*)	0.010–0.105	Undular to breaking	0.50–0.89	1.13–1.47	Rough screens ($k=8$ mm) $L=12$ m, $B=0.5$ m

Note: N/A=not applicable; d_o=initial depth measured at $x=5$ m; F=bore Froude number ($F=(V_o+U)/\sqrt{g\times d_o}$); h=gate opening after gate closure; Q=initial steady flow rate; U=surge front celerity measured at $x=5$ m; (+) at 5.2 m from the gate; and (*) measured above the screens.

range. Both acoustic displacement meters and ADV were synchronized within +/−1 ms and were sampled simultaneously at 200 Hz. In the present study, the unsteady ADV data processing was limited to a removal of communication errors and a replacement by interpolation following Koch and Chanson (2008). The bore front passage was associated systematically with some increase in average signal-to-noise ratios, signal correlations, and, to a lesser extent, signal amplitudes. While these observations were not an objective validation, they tended to support the use of ADV in such a highly unsteady flow situation.

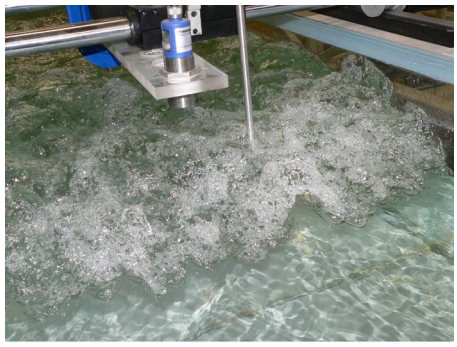

(a)

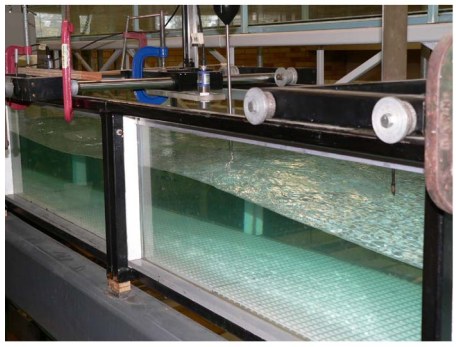

(b)

Fig. 3. Photographs of the tidal bore experiments on smooth and rough inverts: (a) breaking surge advancing on the smooth bed, F=1.50, surge front passing the ADV at $x=5$ m (shutter speed: 1/80 s) (note that the acoustic displacement sensor located above the free surface and sampling the surface elevation immediately above the ADV sampling volume); (b) undular surge propagating on the rough screens, F=1.20 [passage of the first wave crest at $x\sim4.5$ m (shutter speed: 1/80 s); surge propagation from left to right]

The translation of the ADV probe in the vertical direction was controlled by a fine adjustment traveling mechanism connected to a Mitutoyo digimatic scale unit. The error on the vertical position of the probe was $\Delta z<0.025$ mm. The accuracy on the longitudinal position was estimated as $\Delta x<+/-2$ mm. The accuracy on the transverse position of the probe was less than 1 mm. Herein all the measurements were taken on the channel centerline since the earlier work of Koch and Chanson (2005, 2009) showed little transverse differences but close to the sidewall where the acoustic Doppler velocimetry was adversely affected by the sidewall proximity (Chanson et al. 2007).

Inflow Conditions and Bore Generation

Some detailed measurements of the velocity distributions were performed in the steady flow at $x=5$ m. The results showed that the inflow conditions were partially developed (Fig. 4). Some results are presented in Fig. 4 in terms of the time averaged longitudinal velocity component V_x and its standard deviation v'_x. The boundary layer thickness δ was about $\delta/d_o=0.32$ and 0.48 for the experiments Series 1A (smooth PVC) and 1B (rough screens), respectively, where d_o=initial flow depth. The findings were close to and consistent with the earlier study of Koch and Chanson (2009) with a different initial discharge and a smooth bed. For the rough screen invert (Series 1B), the data showed a marked effect of the bed roughness. Some larger turbulent velocity fluctuations were observed above the rough screens, while the vertical distribution of longitudinal velocity exhibited a flatter shape as seen in Fig. 4. The shape was consistent with a fully rough turbulent boundary layer (Schlichting 1960).

The experimental flow conditions were selected to generate both undular (nonbreaking) and breaking bores with the same initial flow rate Q (Table 1). The only dependant parameters were the bed roughness and the downstream gate opening after closure h (Table 1, "Gate opening h (m)"). The steady gradually varied flow conditions were established for at least 3 min prior to measurements. A positive surge was generated by the rapid partial closure of the downstream gate. The gate closure time was less than 0.2 s. After closure, the bore propagated upstream and each experiment was stopped before the bore front reached the intake structure to avoid wave reflection interference. Further information on the experimental facility, instrumentation, boundary conditions, and gate closure were reported in Chanson (2008).

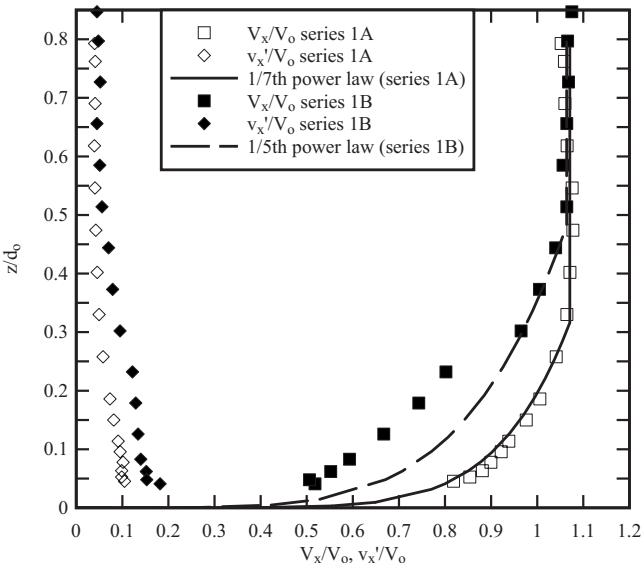

Fig. 4. Initial steady flow conditions: dimensionless vertical distribution of velocity V_x/V_o and turbulent velocity fluctuations v_x'/V_o (at $x=5$ m)

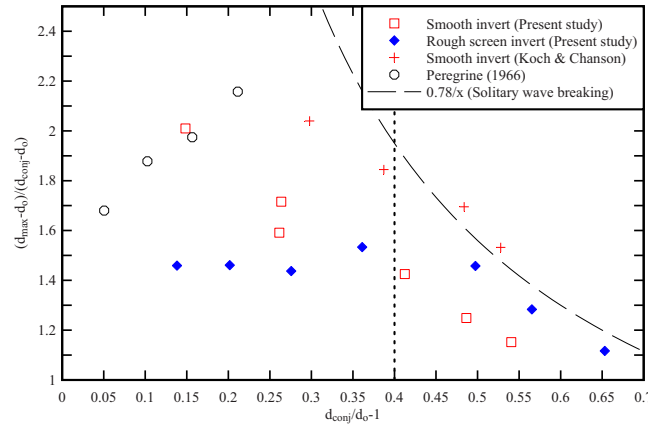

Fig. 5. Maximum wave height of undular bores [comparison between experimental data (Koch and Chanson 2008, present study), calculations (Peregrine 1966), and maximum solitary wave height]

Experimental Observations

Basic Flow Patterns

For the same initial flow conditions, three types of bores were observed: an undular (nonbreaking) bore for surge Froude numbers F less than 1.3, an undular surge with some slight breaking for F between 1.3 and 1.45 to 1.5, and a breaking bore with a marked roller for F greater than 1.45–1.5 (Fig. 3). The same flow patterns were observed with both smooth and rough inverts. The present observations are summarized in Table 2 where they are compared with two earlier studies.

For a small surge Froude number ($F<1.3$), the bore propagated upstream relatively slowly and the front was followed by a train of well-formed undulations: i.e., an undular bore pattern [Fig. 3(b)]. The free-surface undulations had a smooth appearance and no wave breaking wave observed. For $1.2<F$, some small cross waves were seen starting next to the sidewalls upstream of the first wave crest and intersecting next to the first crest. A similar cross-wave pattern was observed in stationary undular hydraulic jumps (Chanson and Montes 1995; Montes and Chanson 1998; Ben Meftah et al. 2007). For intermediate Froude numbers ($1.3<F<1.45-1.5$), some small wave breaking was observed at the leading wave crest, and the secondary waves were flatter. The finding was observed for both smooth and rough beds, and it was consistent with the earlier observations of Koch and Chanson (2008) and Hornung et al. (1995), although the latter study reported some observations for a positive surge propagating in still water. At large surge Froude numbers (i.e., $F>1.45-1.5$), a breaking bore was observed. The surge front propagated relatively rapidly. A well-formed roller was observed and the free-surface appeared to be quasi-two dimensional [Fig. 3(a)].

For the undular (nonbreaking) bore, the maximum wave heights (d_{max}) attained by the undulations are presented in Fig. 5. The maximum wave height was that of the first wave crest and it was limited by breaking. Experimental data were compared with the calculations of Peregrine (1966). The appearance of wave breaking corresponded to $(d_{conj}/d_o-1)>0.4$ or $F>1.5$ (Table 2). That condition is shown in Fig. 4 (thick vertical line) together with the maximum height of a solitary wave (thin dashed line). The experimental results were in general agreement with the solitary wave theory.

Effect of Bed Friction on Undular Bores

For sinusoidal water waves, Ippen and Kulin (1957) developed an estimate for the wave amplitude attenuation due to boundary friction as

Table 2. Experimental Observations of Tidal Bore Types in a Horizontal Rectangular Channel

Reference	S_o	Q (m^3/s)	d_o (m)	Undular bore	Undular bore with breaking	Breaking bore	Remarks
Hornung et al. (1995)	0	0	—	$F<1.6$	$1.6<F<1.9$	$1.9<F$	Smooth bed
Koch and Chanson (2005, 2009)	0	0.040	0.079	$F<1.4-1.5$	$1.5<F<1.7$	$1.7<F$	Smooth PVC bed $B=0.5$ m
Present study							
Series 1A	0	0.058	0.137	$F<1.3$	$1.3<F<1.45$	$1.45<F$	Smooth PVC bed $B=0.5$ m
Series 1B	0	0.058	0.142	$F<1.3$	$1.3<F<1.5$	$1.5<F$	Rough screens ($k=8$ mm) $B=0.5$ m

Note: d_o=initial depth measured at $x=5$ m and F=bore Froude number.

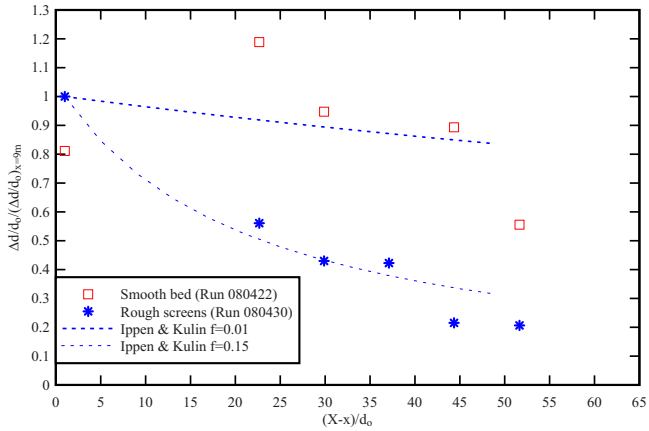

Fig. 6. Attenuation of the wave height for undular bore experiments on smooth and rough bed (F=1.2) (comparison between first wavelength data and theory of Ippen and Kulin 1957 [Eq. (5)])

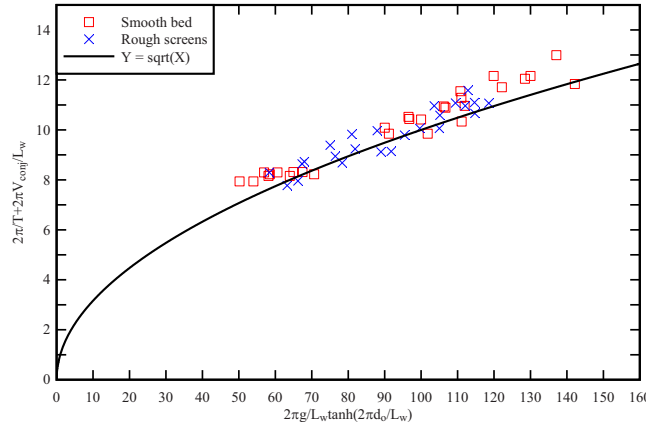

Fig. 7. Wave dispersion in undular bore experiments on smooth and rough bed (comparison with theoretical solution of gravity wave dispersion in intermediate waters [Eq. (7)])

$$\frac{\Delta d/d}{(\Delta d/d)_{x=x_o}} = \left(1 + \frac{2}{15} f \frac{(x_o - x)/d}{\Delta d/d}\right)^{-1} \tag{5}$$

where Δd=attenuated positive wave height at a distance $(x_o - x)$ from the reference location x_o where the wave height is $\Delta d_{x=xo}$; d=water depth measured at x; and f=Darcy-Weisbach friction factor. In the present study, the undular (nonbreaking) bore propagation data showed some attenuation of the wave height Δd with increasing distance of bore propagation. On the smooth bed, the wave attenuation was about 10% over 8.5 m. On the rough screens, the wave attenuation was nearly 70% for F=1.2 (Fig. 6), but it decreased considerably for larger Froude numbers. For F=1.28 and 1.37, the wave attenuation on the rough bed was comparable to the smooth-bed attenuation. Eq. (5) predicted a trend that was comparable to the present data, although it underestimated the effect of rough boundary friction. In Fig. 6, Eq. (5) matched the rough screen data using a friction factor f that was twice the steady flow estimate [Eq. (3)]. Note that Ippen and Kulin (1957) observed similarly a greater effect of boundary friction during their experiments with the smallest water depths.

A different reasoning may derive from the application of the Saint-Venant equations. When a positive surge propagates against a steady flow at near equilibrium conditions, the method of characteristics yields an analytical solution implying that the flow resistance delays the bore formation for $V_o/\sqrt{gd_o} < 2$, and makes the positive surge more dispersive (Henderson 1966). The result is consistent with the above approach and the experimental data, although neither Eq. (5) nor Saint-Venant equation considerations can explain the lesser undular wave attenuation at larger Froude numbers ($1.3 \leq F < 1.5$). The latter might be linked with some local energy dissipation by the light wave breaking at the first wave crest.

The undular wave period and wavelength data were further compared with the wave dispersion theory for gravity waves in intermediate water depths. For a wave propagating upstream in presence of a current with an initial velocity V positive downstream, the linear wave theory yields a dispersion relationship between the angular frequency $2\pi/T$ and wave number $2\pi/L_w$

$$\frac{2\pi}{T} + \frac{2\pi V}{L_w} = \sqrt{\frac{2\pi g}{L_w} \tanh\left(\frac{2\pi d}{L_w}\right)} \tag{6}$$

where L_w=wavelength; T=wave period as seen by an observer fixed on the bank; and d=initially still water depth (Dingemans 1997; Nielsen 2009). For the free-surface undulations of an undular surge propagating against a current with an initial velocity V_o, Eq. (6) becomes

$$\frac{2\pi}{T} + \frac{2\pi V_o}{L_w} = \sqrt{\frac{2\pi g}{L_w} \tanh\left(\frac{2\pi d_{\text{conj}}}{L_w}\right)} \tag{7}$$

where d_{conj}=conjugate depth. Eq. (7) is compared with experimental data in Fig. 7. The data showed close results between smooth and rough bed experiments, as well as with Eq. (7) (Fig. 7). However it must be stressed that Eq. (7) was developed for regular waves rather than for the undular bore secondary waves.

Experimental Results: Turbulent Flow Field

Presentation

The instantaneous velocity measurements demonstrated some major differences in longitudinal velocity redistribution between the undular (nonbreaking) and breaking bores, as previously observed by Koch and Chanson (2009) for different flow conditions. The undular bore was characterized by a train of secondary waves following the leading wave front. No roller was observed. At the ADV sampling point, the passage of the bore front was associated with a relatively gentle longitudinal flow deceleration at all vertical elevations (Fig. 8). In Figs. 8 and 10, V_x=longitudinal velocity component positive downstream; V_y=transverse velocity component positive to left; V_z=vertical velocity component positive upward; and V_o=initial depth-averaged flow velocity. The longitudinal velocity component was minimum beneath the first wave crest and it oscillated afterward with the same period as the surface undulations and out of phase. The vertical velocity data presented a similar oscillating pattern beneath the free-surface undulations with the same periodicity, but out of phase. The irrotational flow theory predicts such a redistribution of the longitudinal and vertical velocities between wave crests and troughs (Rouse 1938; Montes and Chanson 1998). The ideal fluid flow

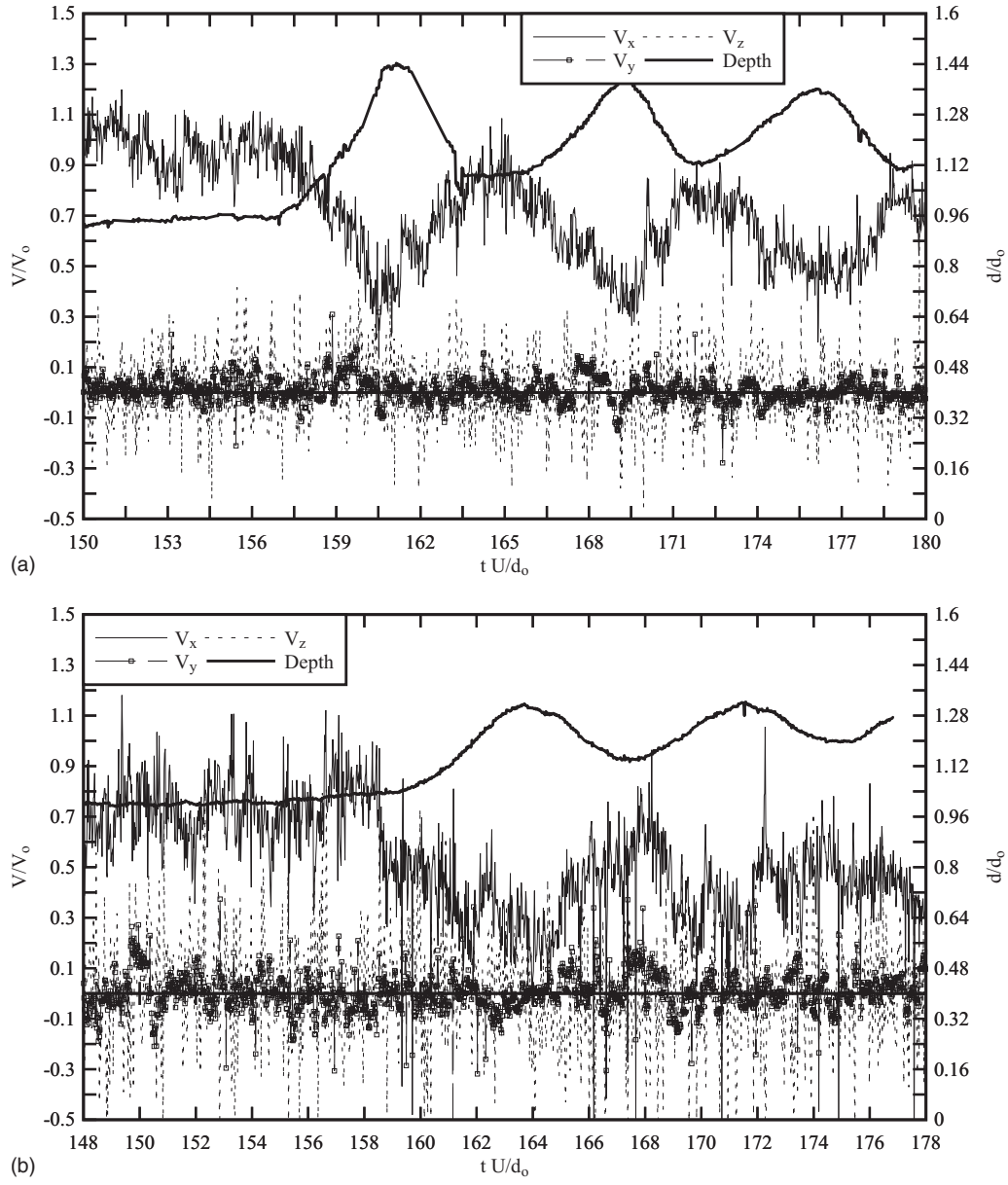

Fig. 8. Dimensionless instantaneous velocity components beneath an undular tidal bore: (a) smooth PVC invert, d_o=0.1385 m, V_o =0.830 m/s, U=0.553 m/s, F=1.17 (Experiment Series 1A), z/d_o=0.150; (b) rough screens, d_o=0.1412 m, V_o=0.826 m/s, U=0.551 m/s, F=1.20 (Experiment Series 1B), z/d_o=0.179

theory shows also that the pressure field is not hydrostatic, with a pressure gradient larger then the hydrostatic pressure gradient ρg beneath the troughs and greater than ρg below the wave crest as sketched in Fig. 9.

In contrast, a breaking bore exhibited a marked roller and some bubble entrainment [Fig. 3(a)]. The data showed that the free-surface elevation rose slowly immediately prior to the roller, with the free-surface curving upwards ahead of the roller toe, as previously observed by Hornung et al. (1995) and Koch and Chanson (2009). This gentle rise of free surface was linked with a gradual decrease of the longitudinal velocity component at all vertical elevations. Immediately after, the passage of the roller was marked by a sharp rise in free-surface elevation corresponding to a discontinuity in terms of the water depth. The passage of the bore front corresponded to a flow deceleration seen in Fig. 10(a). The rate of flow deceleration was notably sharper in a breaking bore than that for an undular bore at the same relative elevation z/d_o. Close to the bed ($z/d_o<0.2$), the longitudinal velocity could become negative although for a short duration highlighting a rapid transient flow separation [Fig. 10(a), for $tU/d_o \sim 1,232.5$]. This flow feature was first reported by Koch and Chanson (2009) and obtained numerically by Furuyama and Chanson (2008).

For all experiments, the turbulent velocity data showed some large fluctuations of all velocity components beneath the bore and in the flow field advected upstream behind the bore. Large time variations of the longitudinal, vertical, and transverse velocity components were seen at all vertical elevations for both undular (nonbreaking) and breaking bores. Similar observations were reported by Hornung et al. (1995) and Koch and Chanson (2008, 2009), although the former study focused on the vorticity of the flow.

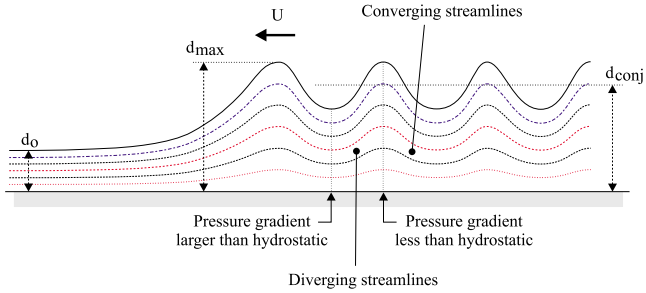

Fig. 9. Instantaneous streamline pattern beneath an undular (nonbreaking) bore for an ideal fluid flow motion

Effect of Bed Roughness

The experimental observations showed that the rough invert had a drastic impact on the turbulent flow field. The initial flow exhibited higher turbulence levels at all vertical elevations (Fig. 4). For an undular bore, the bed roughness induced a strong attenuation of the oscillating free-surface flow pattern effect on the longitudinal and vertical velocity components next to the bed ($z/d_o < 0.2$) [Fig. 8(b)], although the oscillating pattern was still seen in the upper flow region ($z/d_o > 0.5$). With a breaking bore, the longitudinal velocity data indicated a longer transient recirculation next to the bed ($z/d_o < 0.2$) [Fig. 10(b)]. Such a recirculation pattern is sketched in Fig. 2 and it was not associated with any irregularity of the movement of the roller toe. In the recirculation region, large negative longitudinal velocities were observed: $V_x/V_o \sim -0.3$ to -0.5 typically [e.g., Fig. 10(b)]. The transient event lasted at least 3 s. Its precise duration was possibly longer

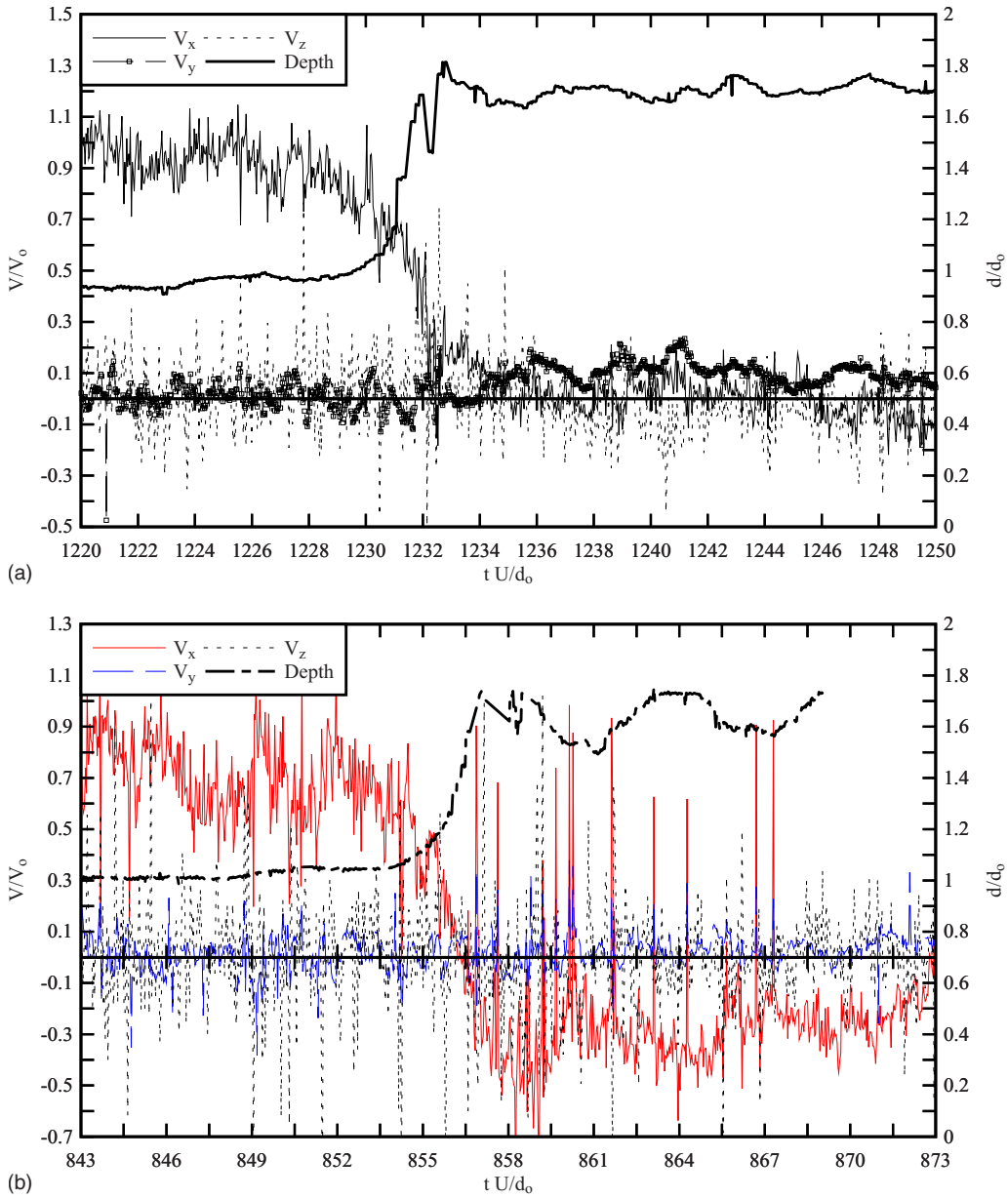

Fig. 10. Dimensionless instantaneous velocity components beneath a breaking tidal bore: (a) smooth PVC invert, d_o=0.1388 m, V_o=0.832 m/s, U=0.903 m/s, F=1.50 (Experiment Series 1A), z/d_o=0.150; (b) rough screens, d_o=0.1415 m, V_o=0.824 m/s, U=0.892 m/s, F=1.46 (Experiment Series 1B), z/d_o=0.179

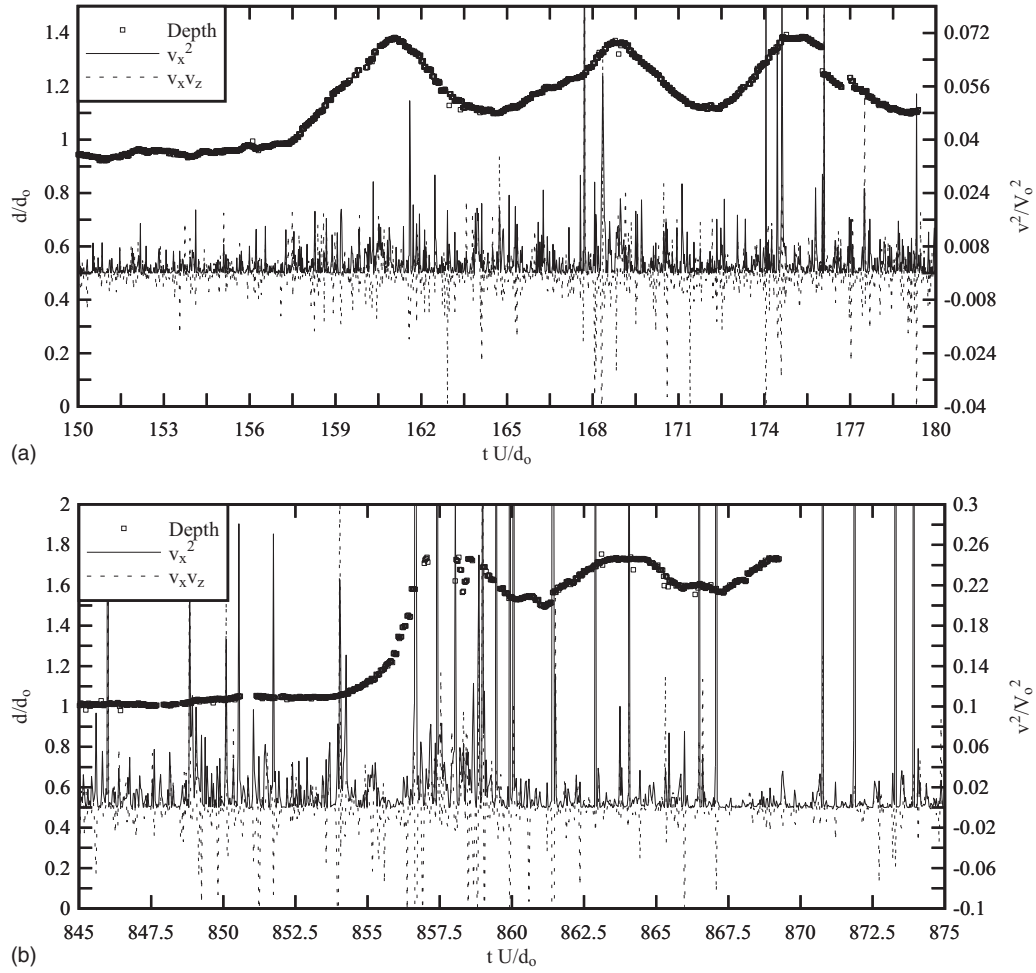

Fig. 11. Dimensionless instantaneous turbulent stresses v_x^2/v_o^2 and $v_x \times v_z/V_o^2$ beneath bores: (a) undular (nonbreaking) bore on smooth horizontal invert: d_o=0.1385 m, V_o=0.830 m/s, U=0.553 m/s, F=1.17 (Experiment Series 1A), z/d_o=0.764; (b) breaking bore on rough screen invert: d_o=0.1415 m, V_o=0.824 m/s, U=0.892 m/s, F=1.46, S_o=0 (Experiment Series 1B), z/d_o=0.179

because the data collection was stopped as soon as the surge front reached the upstream channel end (x=0). Although the bed roughness seemed to enhance the transient recirculation, this recirculation pattern was a flow feature specific to the breaking bore. No such recirculation was observed beneath the undular (nonbreaking) bore.

Turbulent Shear Stresses

The instantaneous turbulent stresses were calculated using a variable interval time average technique (Koch and Chanson 2008). The tidal bore passage was characterized by large fluctuations in Reynolds stresses (Fig. 11). Fig. 11 presents some unsteady Reynolds stress data beneath a tidal bore. Fig. 11(a) corresponds to an undular (nonbreaking) bore on a smooth invert and Fig. 11(b) to a breaking bore on a rough screen invert. In each figure, the graph presents the time variation of the dimensionless Reynolds stresses v_x^2/v_o^2 and $v_x \times v_z/V_o^2$, and water depth d/d_o, where v=turbulent velocity; the subscripts x and z refer, respectively, to the longitudinal and vertical velocity components; and t=time.

The experimental measurements showed some large fluctuating turbulent stresses below the bore front and in the flow behind. The Reynolds stress levels were significantly larger than before the surge passage, and large normal and tangential stresses were observed. In an undular tidal bore, some large Reynolds stresses were recorded beneath the secondary waves suggesting the long-lasting sediment mixing beneath these "whelps" (Chanson 2005; Koch and Chanson 2008). With the breaking surge, some large shear stresses and Reynolds stress fluctuations were observed during the roller passage and shortly after, especially in the upper flow region (z/d_o>0.5). It is believed that these large turbulent stresses were caused by the proximity of the developing mixing layer of the roller sketched in Fig. 2. A comparison between undular and breaking bores showed that (1) the magnitude of turbulent stresses was comparable, but (2) the large fluctuations in Reynolds stresses lasted for a significantly longer period beneath

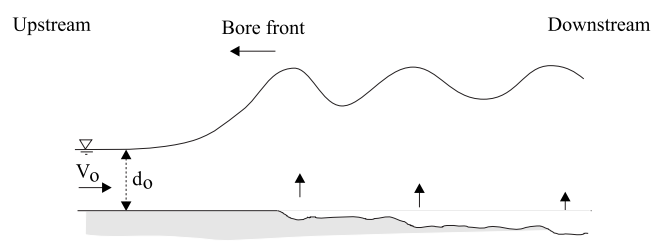

Fig. 12. Sketch of bed scour and sediment erosion beneath the successive undulations of an undular (nonbreaking)

the undular bore. The finding implied that the undular tidal bores may contribute to significant bed scour in tidal bore affected estuaries as sketched in Fig. 12.

Discussion

A number of similar features were observed on both smooth and rough inverts. The velocity measurements indicated the existence of energetic turbulent events beneath and after the tidal bore front (Figs. 8 and 10). These were best seen by some sudden and rapid fluctuations of the transverse and vertical velocity data as well as with significant fluctuations of the Reynolds stresses. The duration of these turbulent "patches" seemed greater beneath an undular bore, while these were more focused and shorter beneath a breaking bore. Such vigorous and energetic turbulent events were some form of macroturbulence that is likely induced by secondary motion. In a natural, nonprismatic channel, some vorticity may be generated additionally by the invisicid flow motion and complicated secondary currents may develop (Thorne and Hey 1979; Trevethan et al. 2008). The large-scale turbulence maintained its coherence as the tidal bore propagates upstream. In the Daly River (Australia), such a period of very strong turbulence was observed about 20 min after the bore passage that lasted for about 3 min: "*about 20 min after the passage of the undular bore, a 3-min-duration patch of macro-turbulence was observed. […] This unsteady motion was sufficiently energetic to topple moorings that had survived much higher, quasi-steady currents of 1.8 m/s*" (Wolanski et al. 2004). The anecdote suggested the upstream advection of a "cloud" of turbulence and vorticity behind the tidal bore for possibly a considerable distance. The advection speed of the turbulence boils was slower than the tidal bore celerity, explaining possibly the 20-min delay.

Conclusions

Limited quantitative information is available to date on the turbulence induced by tidal bores because the turbulent flow field had rarely been studied with a fine instrumentation under well-defined flow conditions. Herein new experiments were conducted in a large rectangular channel to study specifically the effects of bed roughness, and detailed velocity measurements were performed with a high temporal and spatial resolution (200 Hz, sampling volume size: 1.5 mm) while the free-surface elevations were recorded using nonintrusive acoustic displacement meters. The range of experimental investigations encompassed undular (nonbreaking) and breaking bores on both smooth and rough invert conditions (Table 1).

A undular (nonbreaking) bore was observed for F less than 1.45 to 1.5, when the wave front was followed by a train of well-defined secondary waves in estuaries. For $F > 1.5$, a breaking bore was observed with a marked roller. The instantaneous velocity measurements showed a rapid flow deceleration at all vertical elevations, and some large fluctuations of all velocity components were recorded beneath the surge and whelps. The turbulent Reynolds stress data highlighted the large normal and tangential stresses beneath the surge front. A comparison between undular and breaking surge data suggested some basic differences. In a breaking bore, some large turbulent stresses were observed next to the shear zone in a region of high velocity gradients. Next to the bed, however, some transient flow recirculation was recorded. In an undular bore, the large velocity fluctuations and Reynolds stresses were recorded beneath the first wave crest and the secondary waves implying a long-lasting effect after the bore front passage. A systematic comparison was conducted to study the effects of bed roughness. The boundary friction contributed to some wave attenuation and dispersion, and the free-surface data showed some agreement with the wave dispersion theory for intermediate gravity waves. The instantaneous velocity data indicated also a marked effect of the rough screens on the turbulent velocity field, especially close to the bed ($z/d_o < 0.2$) for both undular and breaking bores.

Overall the experimental findings were consistent with the field observations and anecdotal evidences. These showed in particular the significant impact of undular (nonbreaking) bores and their potential impact on natural ecosystems. The present results demonstrated that a tidal bore remains a challenging research topic to theoreticians. In a breaking tidal bore, the transient recirculation observed next to the bed remained unexplained. In the field, tidal bores in natural systems propagate over a movable bed. How does bed erosion take place? Is Fig. 12 representative of the real world?

Acknowledgments

The writer acknowledges the technical assistance of Graham Illidge and the helpful discussion with Dr. Peter Nielsen.

References

Barré de Saint Venant, A. J. C. (1871). "Théorie et Equations Générales du Mouvement Non Permanent des Eaux, avec Application aux Crues des Rivières et à l'Introduction des Marées dans leur Lit (2ème Note) [Theory and equation of unsteady open channel flows, with applications to river floods and tidal influence (2nd Note)]. Comptes Rendus des séances de l'Académie des Sciences, Paris, France." *Séance*, 73, 237–240.

Ben Meftah, M., De Serio, F., Mossa, M., and Pollio, A. (2007). "Analysis of the velocity field in a large rectangular channel with lateral shockwave." *Environ. Fluid Mech.*, 7(6), 519–536.

Benet, F., and Cunge, J. A. (1971). "Analysis of experiments on secondary undulations caused by surge waves in trapezoidal channels." *J. Hydraul. Res.*, 9(1), 11–33.

Benjamin, T. B., and Lighthill, M. J. (1954). "On cnoidal waves and bores." *Philos. Trans. R. Soc. London, Ser. A*, 224(1159), 448–460.

British Standard. (1943). "Flow measurement." *British standard code BS 1042:1943*, London.

Chanson, H. (2004). *The hydraulics of open channel flow: An introduction*, 2nd Ed., Butterworth-Heinemann, Oxford, U.K.

Chanson, H. (2005). "Mascaret, Aegir, Pororoca, Tidal Bore. Quid? Où? Quand? Comment? Pourquoi? (Mascaret, Aegir, Pororoca, Tidal Bore. What? Where? When? How? Why?" *Houille Blanche*, (3), 103–114.

Chanson, H. (2008). "Turbulence in positive surges and tidal bores. Effects of bed roughness and adverse bed slopes." *Hydraulic Model Rep. No. CH68/08*, Div. of Civil Engineering, The Univ. of Queensland, Brisbane, Australia.

Chanson, H., and Montes, J. S. (1995). "Characteristics of undular hydraulic jumps. Experimental apparatus and flow patterns." *J. Hydraul. Eng.*, 121(2), 129–144.

Chanson, H., Trevethan, M., and Koch, C. (2007). "Turbulence measurements with acoustic Doppler velocimeters." *J. Hydraul. Eng.*, 133(11), 1283–1286.

Darcy, H. P. G., and Bazin, H. (1865). *Recherches Hydrauliques. Imprimerie Impériales, Paris, France, Parties 1ère et 2ème*.

Darwin, G. H. (1897). "The tides and kindred phenomena in the solar

system." *Lectures delivered at the Lowell Institute, Boston*, W.H. Freeman and Co. Publ., London.

Dingemans, M. W. (1997). *Water wave propagation over uneven bottoms. Advanced series on ocean engineering*, Vol. 13, World Scientific, Singapore, Singapore.

Favre, H. (1935). *Etude Théorique et Expérimentale des Ondes de Translation dans les Canaux Découverts* (Theoretical and Experimental study of travelling surges in open channels), Dunod, Paris, France.

Furuyama, S., and Chanson, H. (2008). "A numerical study of open channel flow hydrodynamics and turbulence of the tidal bore and dam-break flows." *Hydraulic Model Rep. No. CH66/08*, Div. of Civil Engineering, The Univ. of Queensland, Brisbane, Australia.

Henderson, F. M. (1966). *Open channel flow*, MacMillan, New York.

Hornung, H. G., Willert, C., and Turner, S. (1995). "The flow field downstream of a hydraulic jump." *J. Fluid Mech.*, 287, 299–316.

Ippen, A. T., and Kulin, G. (1957). "The effect of boundary resistance on solitary waves." *Houille Blanche*, 12(3), 390–400.

Koch, C., and Chanson, H. (2005). "An experimental study of tidal bores and positive surges: Hydrodynamics and turbulence of the bore front." *Hydraulic Model Rep. No. CH56/05*, Dept. of Civil Engineering, The Univ. of Queensland, Brisbane, Australia.

Koch, C., and Chanson, H. (2008). "Turbulent mixing beneath an undular bore front." *J. Coastal Res.*, 24(4), 999–1007.

Koch, C., and Chanson, H. (2009). "Turbulence measurements in positive surges and bores." *J. Hydraul. Res.*, 47(1), 29–40.

Liggett, J. A. (1994). *Fluid mechanics*, McGraw-Hill, New York.

Mazumder, N. C., and Bose, S. (1995). "Formation and propagation of tidal bore." *J. Waterway, Port, Coastal, Ocean Eng.*, 121(3), 167–175.

Montes, J. S., and Chanson, H. (1998). "Characteristics of undular hydraulic jumps. Results and calculations." *J. Hydraul. Eng.*, 124(2), 192–205.

Nielsen, P. (2009). *Coastal and estuarine processes*, World Scientific, Singapore, Singapore.

Peregrine, D. H. (1966). "Calculations of the development of an undular bore." *J. Fluid Mech.*, 25, 321–330.

Rayleigh, L. (1908). "Note on tidal bores." *Philos. Trans. R. Soc. London, Ser. A*, 81(541), 448–449.

Rouse, H. (1938). *Fluid mechanics for hydraulic engineers*, McGraw-Hill, New York.

Schlichting, H. (1960). *Boundary layer theory*, 4th Ed., McGraw-Hill, New York.

Thorne, C. R., and Hey, R. D. (1979). "Direct measurements of secondary currents at a river inflexion point." *Nature*, 280, 226–228.

Treske, A. (1994). "Undular bores (Favre-waves) in open channels—Experimental studies." *J. Hydraul. Res.*, 32(3), 355–370.

Trevethan, M., Chanson, H., and Brown, R. (2008). "Turbulence characteristics of a small subtropical estuary during and after some moderate rainfall." *Estuarine Coastal Shelf Sci.*, 79(4), 661–670.

Tricker, R. A. R. (1965). *Bores, breakers, waves and wakes*, Elsevier, New York.

Wolanski, E., Williams, D., Spagnol, S., and Chanson, H. (2004). "Undular tidal bore dynamics in the Daly estuary, northern Australia." *Estuarine Coastal Shelf Sci.*, 60(4), 629–636.